Scientific Research Publishing

Open Journal of Geology, 2023, 13, 783-805
https://www.scirp.org/journal/ojg
ISSN Online: 2161-7589
ISSN Print: 2161-7570

Estimation of Aquifer Transmissivity Using Dar Zarrouk Parameters at Ogbozara-Ekwegbe-Agu and the Environ, Enugu State, Nigeria

Charles Chibueze Ugbor, Ugochukwu Kingsley Ogbodo*

Department of Geology, University of Nigeria, Nsukka, Nigeria
Email: *ugomsinachiogbodo@gmail.com

How to cite this paper: Ugbor, C.C. and Ogbodo, U.K. (2023) Estimation of Aquifer Transmissivity Using Dar Zarrouk Parameters at Ogbozara-Ekwegbe-Agu and the Environ, Enugu State, Nigeria. *Open Journal of Geology*, **13**, 783-805.
https://doi.org/10.4236/ojg.2023.138035

Received: May 4, 2023
Accepted: July 30, 2023
Published: August 2, 2023

Abstract

This study was undertaken to determine the hydrologic properties of the aquifer materials at Ogbozara-Opi/Ekwegbe-Agu and environs by the estimation of the aquifer transmissivity using Dar Zarrouk parameters. The study area lies in the Anambra basin and is underlain, from bottom to top, by 3 prominent geologic formations; Enugu Formation, Mamu Formation and Ajali Formation respectively. A total of 19 sounding stations were occupied within the study area using the Ohmega resistivity meter. The VES data were interpreted using the conventional partial curve matching technique to obtain initial model parameters which were later used as input data for computer iterative modelling using the Interpex software. These analyses were further combined with information from two existing boreholes in the study area to estimate aquifer hydraulic parameters using Dar-Zarrouk parameters. The layer parameters thus obtained revealed that the dominant curve type obtained from the different formations is the AK curve type followed by the HK curve type. An average of 6 geo-electric layers were delineated across all transect taken with resistivity values ranging from 25.42 - 105.85 Ωm, 186.38 - 3383.3 Ωm and 2992.3 - 6286.4 Ωm in the Enugu, Mamu and Ajali Formations respectively. Results of the study revealed the aquifer resistivity in the study area ranges from 1 - 500 Ωm. The depth to the water table range from 13 - 208 m with a mean value of 76.05, while aquifer thickness varies between 95 and 140 m with a mean value of 102.89 m. The values of the Dar-Zarrouk parameters revealed that the transverse resistance varies between −10,000 - 170,000 Ωm^2, while the longitudinal conductance varies from 0.1 - 1 to 1.9 Ω - 1. Similarly, the hydraulic conductivity in the area ranges from 5 to 50 m/day, while the transmissivity values range from 1000 to 14,000 m^2/day.

Keywords

Aquifer, Dar Zarrouk Parameters, VES, Transmissivity, Conductance

1. Introduction

The sedimentary sequences of Southeastern Nigeria are known to contain several aquiferous units [1]. Several authors have over the years successfully estimated aquifer hydraulic characteristics from Dar-Zarrouk parameters in many parts of Southeastern Nigeria from surface electrical resistivity sounding data [2]. The concept of Dar Zarrouk parameters was first proposed by [3], this postulation holds from the fact that, when the thickness and resistivity of a lithologic subsurface layer is known, its transverse resistance (R) and longitudinal conductance (S) can be calculated easily. Hence their correlative resistivities can be determined. Dar Zarrouk parameters have since been used in the estimation of the hydraulic properties of aquifers. Reference [4] used the concept of Dar zarrouk parameters to estimate the transmissivity of Ajali Sandstone aquifers in southeastern Nigeria. Reference [5] applied the concept of Dar Zarrouk parameters for estimating aquifer hydraulic properties in Enugu State. Reference [6] applied the concept in estimating aquifer hydraulics and delineation of groundwater quality zones. Reference [7] also applied the same concept in a low permeability formation for aquifer hydraulic characteristics. These aquifer hydraulic characteristics are necessary for the management of groundwater resource. The parameters necessary for the description of the dynamics of aquifer, include, geometry of the pore space, geometry of the rock particles, secondary geologic processes such as faulting and folding and secondary deposition These parameters jointly affect the rate and pattern of groundwater flow [8]. Dar Zarrouk and other geoelectric parameters can be used to recognize and differentiate areas of fresh groundwater aquifers from those of saline groundwater. Water can move through soil as saturated flow, unsaturated flow, or fluid flow [9] [10]. Hydraulic conductivity is one of the hydraulic properties of the soil which can be used to determine the behaviour of the soil fluid within the soil system under specified conditions. Hydraulic conductivity determines the ability of the soil fluid to flow through the soil matrix system under a specified hydraulic gradient [11]. Physical characteristics of aquifers such as hydraulic conductivity and transmissivity that control groundwater flow and transport are very important properties and are usually estimated for groundwater flow model calibration. Also these parameters are also important properties for the assessment of contaminated land, and for safe construction of civil engineering structures [12]. It is against this background that this study seeks to determine the hydrologic properties of the aquifer materials in Ogbozara Opi/Ekwegbe-Agu and environ using Dar Zarrouk Parameters.

Geology of the Study Area

The study area, shown in **Figure 1**, lies in Anambra Basin and is underlain from bottom to top by three prominent geologic Formations; Enugu Formation, Mamu Formation and Ajali Formations respectively. The Enugu Formation is made up of carbonaceous shales with the upper half deposited in lower floodplain and swampy environments, and overlie the Nkporo Group [13]. The Mamu

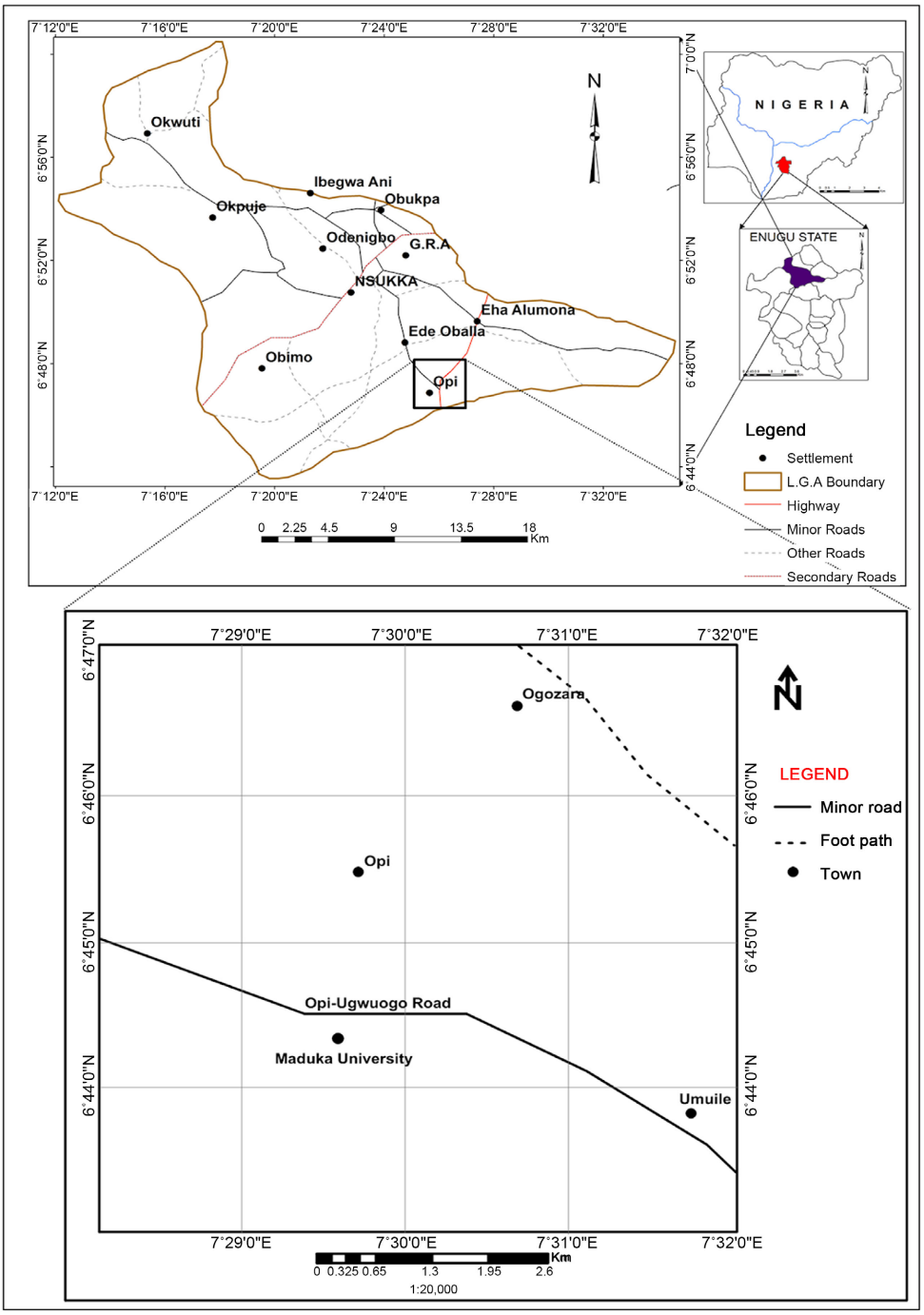

Figure 1. Location and accessibility map of the study area produced by the authors for this study.

Formation, which used to be called the Lower Coal Measures, has marine intercalations made of ammonite-containing shales [14]. Also Reference [15] noted that the sediment pile varies across the Anambra basin and ranges from 75 to over 1000 meters in different parts of the basin. The lithology of the Mamu Formation varies from fine-medium grained, white to grey sandstones, shaley sandstones, sandy shales, grey mudstones, shales and coal seams [16]. The fine grained sandstone unit of the Mamu Formation provides the shaley impermea-

ble base on which the aquifer in the Ajali Formation is laid. The Ajali formation overlies the Mamu formation and it is often referred to as the "False-Bedded Sandstone" Reference [17] and the type locality of the Ajali Formation is in the valley of the Ajali River near Enugu [18]. The Ajali Formation is mostly loose, poorly sorted, coarse-to-fine-grained, poorly cemented sandstone, mudstone, and siltstone, and it dates from the middle to late Maastrichtian Ajali Formation is found within the study area and it is covered by a thick layer of red earthy sands that were formed by weathering and ferruginization. The thickness of this layer varies from less than 300 meters to more than 1000 meters in the middle of the basin [18] [19]. Cross-bedded sedimentary structures are commonly observed on the sands of the Ajali Formation within the study area. These structures are encountered near reactivation surfaces, mud drapes, tidal bundles, backflow ripple channels cut and lateral accretion surfaces [13].

2. Materials and Method of Study

2.1. Materials

The equipment used in this study include Abem Terrameter SAS 300S for the acquisition of vertical electrical sounding data, and Interpex software for interpretation of the sounding data and Borehole data for integration into the data for Dar-Zarouk model building

2.2. Methods of Study

2.2.1. Electrical Resistivity Method

The Vertical electrical sounding (VES) technique which is known to have superior vertical sensitivity according to Reference [20] was adopted to determining the depth variation in apparent resistivity. The potential electrodes were stationary along the traverse while the current electrodes were symmetrically expanded about a fixed central point and readings indicating vertical thickness variations were taken at discrete locations along the profile using the Ohmega resistivity metre.

However, for very large current electrode separation, the electro-potential distance was increased in order to maintain a measurable potential. A total of nineteen (19) VES were taken within the study area. Of these, eight (8), ten (10) and one (1) VES station, respectively, were run within the Ajali, Mamu and Enugu formations in the study area (see **Figure 2**). The VES stations are well distributed within the entire area. The underlying formation for all VES points located within each formation and the summary of the aquifer geo-electric parameters is presented in **Table 1**.

To achieve this, established standard procedure was followed. The data obtained from the VES stations were imported into Interpex and the parameters, resistivity, thickness and depth, of a geo-electric model, thought to be closer to reality (sub-surface resemblance) were estimated, substituted in the aforementioned computer program, edited by trial and error until a very close match was

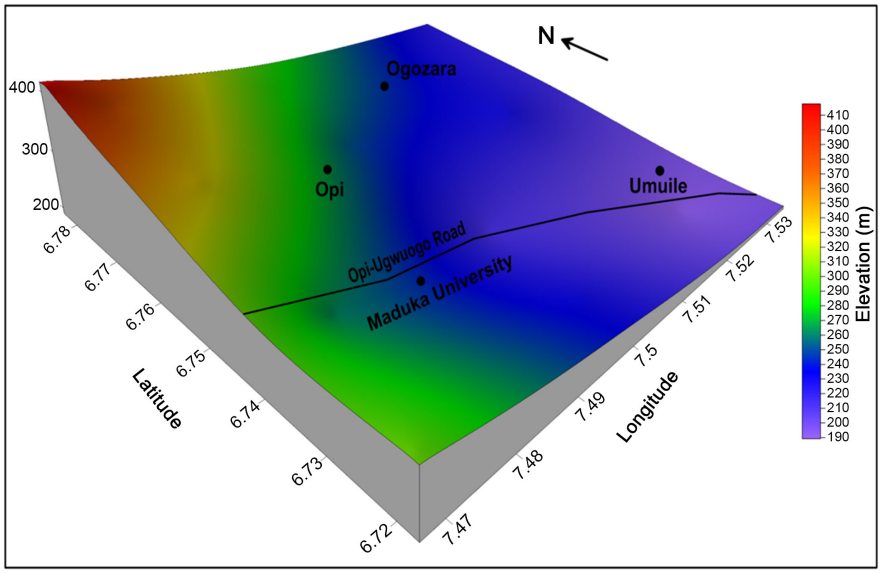

Figure 2. Digital Elevation Model of the study area.

Table 1. Aquifer geo-electric layer parameters obtained from the VES models (ND: No Data).

VES No.	Northing	Easting	Curve Type	No. of Geo-Electric Layers	Water Table (m) (Approx.)	Aquifer Thickness (m) (Approx.)	Aquifer Resistivity (Ωm)
1	6˚44'47.26"N	7˚29'30.22"E	AK	6	31	58	202.860
2	6˚45'12.02"N	7˚29'28.52"E	AK	6	22	85	110.050
3	6˚45'13.16"N	7˚28'14.41"E	HK	6	38	37	113.340
4	6˚46'12.42"N	7˚29'18.21"E	HK	6	30	133	1163.100
5	6˚44'14.18"N	7˚28'47.24"E	HK	6	13	42	56.079
6	6˚44'30.09"N	7˚28'09.43"E	HKA	6	35	60	129.420
7	6˚44'28.32"N	7˚29'50.89"E	QK	7	33	45	94.276
8	6˚44'30.29"N	7˚30'43.23"E	HK	6	14	68	429.730
9	6˚45'23.01"N	7˚30'45.03"E	KHQ	6	82	126	141.910
10	6˚45'27.09"N	7˚31'35.47"E	KHQ	7	81	79	51.475
11	6˚45'15.34"N	7˚29'50.29"E	K	6	74	57	78.777
12	6˚45'57.26"N	7˚29'0.16"E	KA	6	26	31	33.174
13	6˚44'40.11"N	7˚31'16.14"E	K	6	123	81	205.120
14	6˚46'34.48"N	7˚24'26.20"E	HKA	6	36	59	77.553
15	6˚43'56.20"N	7˚30'36.12"E	AK	4	208	ND	7351.900
16	6˚45'27.24"N	7˚28'20.09"E	AK	4	136	ND	2216.200
17	6˚45'21.14"N	7˚28'58.36"E	AK	4	136	ND	64.091
18	6˚45'52.41"N	7˚28'18.21"E	H	6	204	ND	33.884
19	6˚43'01.39"N	7˚30'35.06"E	H	6	123	81	45.667

attained between the calculated and observed resistivity. The exported curves were displayed on a log-log paper in terms of distance and depth and the range of resistivity values after graduation was used to mark distinct stratigraphic layers in each transect. These stratigraphic curves were interpreted quantitatively to determine the nature of the underlying geological formations, presented with its possible geological meanings, resistivity values and layer thicknesses.

2.2.2. Aquifer Characterization Based on Dar Zarouk Parameters

Dar Zarrouk parameters comprise the layer resistivity (ρ) and the thickness (h). The parameters can be used directly in aquifer protection studies and also for the evaluation of hydrologic properties.

2.2.3. Transverse Resistance (R_T) and Longitudinal Conductance (L_C)

If the thickness and resistivity of a lithologic subsurface layer is known, its transverse resistance (T_R) and longitudinal conductance (L_C) can be easily calculated.

For a sequence of horizontal, homogeneous and isotropic layers of resistivity i and thickness h_i, the longitudinal conductance L_C and transverse resistance T_R are defined as follows:

$$L_C = \sum_{i=1}^{n} h_{ii} = h_{11} + h_{22} + h_{33} + \cdots + h_{nn} \tag{1}$$

$$R_T = \sum_{i=1}^{N} ih_i = h_1 + 2h_2 + 3h_3 + \cdots + nh_n \tag{2}$$

Hence, for a single horizontal, homogeneous and isotropic layers, the longitudinal conductance and transverse resistance becomes:

$$L_C = h \tag{3}$$

$$R_T = \rho h \tag{4}$$

where R_T = Transverse resistance ($\Omega \cdot m^2$), ρ = resistivity ($\Omega \cdot m$), h = thickness of layer (m), and L_C = Longitudinal conductance (mho)

2.2.4. Transmissivity (T) and Hydraulic Conductivity (K)

From Darcy's law, the relationship between transmissivity and hydraulic conductivity is given as:

$$T = Kh \tag{5}$$

where T = Transmissivity (m^2/day), K = Hydraulic conductivity (m/day), and h = thickness of layer (m).

Making h subject of the formula in Equations (28) and (29) and substituting in Equation (30), gives:

$$T = KR_T \tag{6}$$

$$T = KL_C \tag{7}$$

Based on the concept of clay content, hydraulic conductivity of clayey sediment could be related to electrical resistivity and according to Reference [21], high clay content generally corresponds with low resistivity and hydraulic conductivity. This implies that in a clay rich aquifer, hydraulic conductivity is directly proportional to resistivity. Hence,

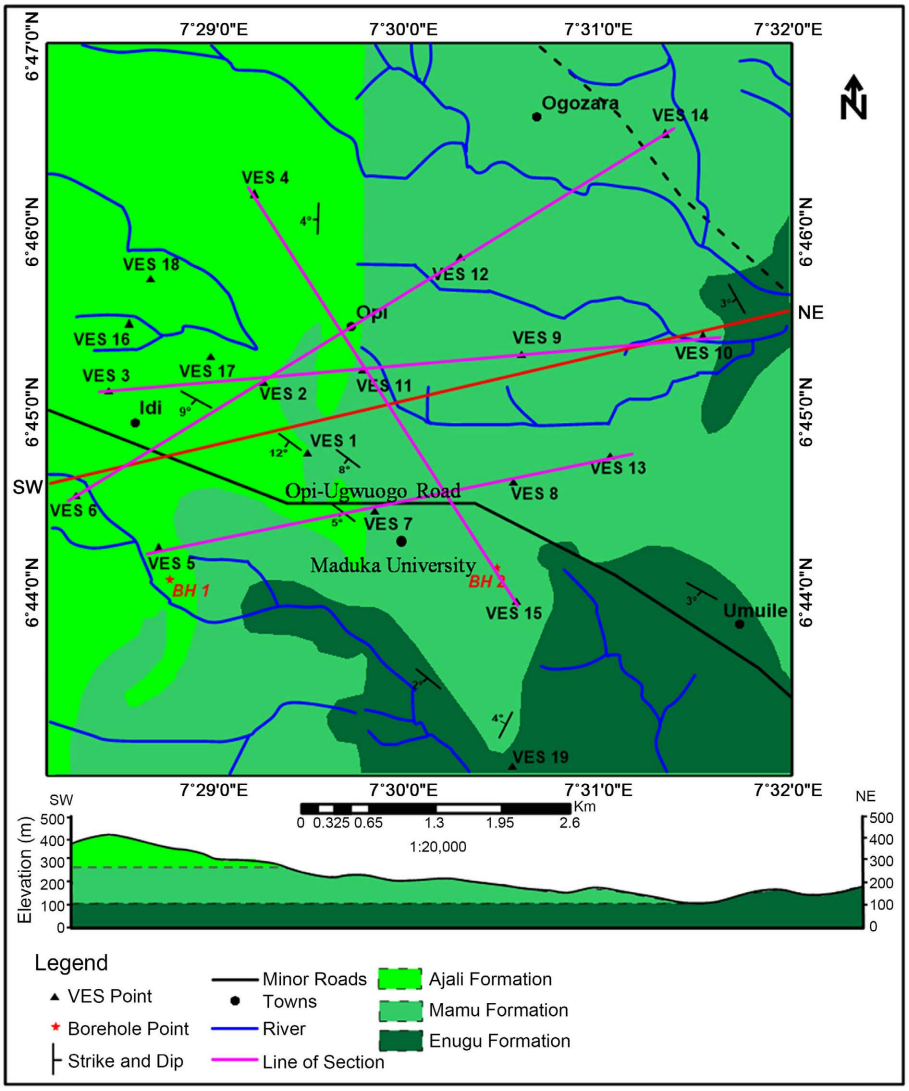

Figure 3. Geological map showing the locations of VES stations within the study area.

$$K = C_1 \tag{8}$$

where C_1 is a constant.

However, in an unconsolidated, sandy aquifer, *i.e.* clay-free aquifer, hydraulic conductivity (K) and porosity ($\emptyset$) have a direct relationship. Inverse relationship exist between porosity and resistivity ($\emptyset \infty 1$) [11]. Therefore,

$$K\rho = C_2 \tag{9}$$

From Equation (8) and Equation (9), it can be deduced that changes in resistivity and hydraulic conductivity across an aquifer are controlled by either variation in effective porosity or changes in clay content.

Substituting Equation (8) into Equation (6) and Equation (7) into Equation (9), gives transmissivity as follows:

$$T = R_T C_1 \tag{10}$$

$$T = L_C C_2 \tag{11}$$

3. Results

3.1. Interpretation of VES Data: 1-D Electro-Stratigraphic Models

The electro-stratigraphic model curves were obtained from the nineteen (19) VES data acquired in the study area in order to better understand the intricate physical properties of the underlying rocks beneath each sounding site and to ascertain key geophysical parameters characterizing each local subsurface structure. The underlying stratigraphic packages for all VES points located within each formation are displayed graphically in Figures 4(a)-(d), Figures 5(a)-(d), Figures 6(a)-(d). The results showing a summary of the aquifer geo-electric parameters is presented in Table 1.

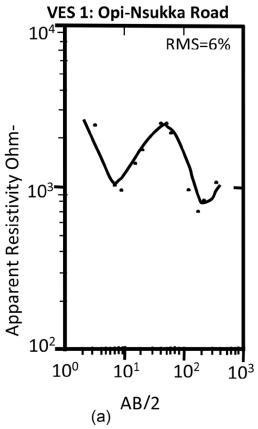

Resistivity Model Interpretation				
PROFILE NO:	VES 1	Opi-Nsukka Roa		
Surface Elevation (m)		244 m		
S/N	Rho	Thick.(m)	Depth (m)	Elev(m)
1	2831.4	1.4355	1.4355	242.56
2	711.21	5.1441	6.5796	237.42
3	5068.2	24.054	30.6336	213.37
4	202.85	57.634	88.2676	155.73
5	6103.8	67.337	155.605	79.336
6	3561			

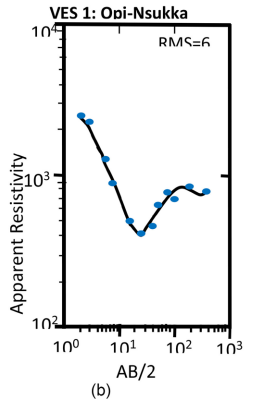

Resistivity Model Interpretation				
PROFILE NO:	VES 7	Opi-Nsukka Road		
Surface Elevation (m)		246		
S/N	Rho	Thick.(m)	Depth(m)	Elev.(m
1	2831.4	1.6604	1.6604	24434
2	928.97	5.7289	7.3893	238.61
3	120.23	7.2325	14.6218	231.38
4	5180.8	18.782	33.4038	212.6
5	94.275	45.192	78.5958	167.4
6	13038	119.86	198.456	47.549
7	11508			

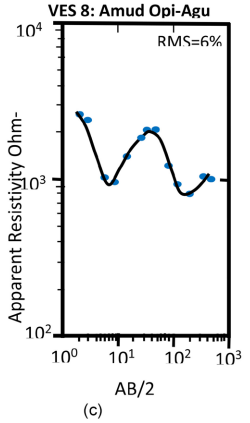

Resistivity Model Interpretation				
PROFILE NO:	VES 8	Amuda Opi-Agu		
Surface Elevation:		246		
S/N	Rho	Thick.	Depth	Elev
1	3365.3	1.6804	1.6804	244.34
2	207.78	1.4303	3.1107	242.86
3	542.5	11.067	14.1777	231.8
4	429.73	67.875	82.0527	153.83
5	1384.5	125.51	207.563	33.317
6	1111.7			

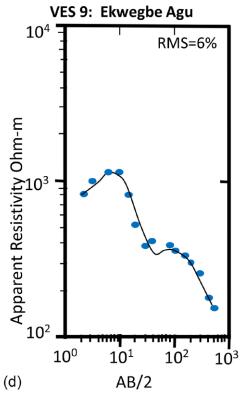

Resistivity Model Interpretation				
PROFILE NO:	VES 9	Amuda Opi-Agu		
Surface Elevation (m)		246		
S/N	Rho	Thick.(m)	Depth (m)	Elev (m)
1	753.15	1.8804	1.8804	243.34
2	1863.9	4.829	6.7094	238.51
3	155.88	9.2215	15.9309	229.29
4	437.51	66.362	82.2929	162.93
5	141.91	125.61	207.903	37.317
6	130.86			

Figure 4. (a-d) Resistivity sounding curve showing geo-electric parameters beneath VES 1 and VES 7 - 9 drawn within Mamu Formation in the northeastern and southeastern parts of the study area.

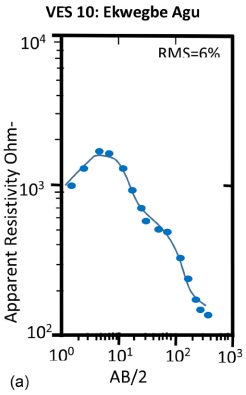

Resistivity Model Interpretation				
PROFILE NO:	VES 10	Amuda Opi-Agu		
Surface Elevation (m)		246		
S/N	Rho	Thick.(m).	Depth (m)	Elev(m
1	712.56	1.8804	1.8804	221.3
2	3124.6	3.1943	5.0747	218.14
3	243.83	4.6023	9.677	213.54
4	506.82	71.483	81.16	142.06
5	51.475	79.083	160.243	62.371
6	220.8	134.14	294.383	71.171
7	147.1			

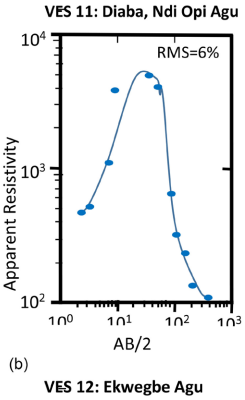

Resistivity Model Interpretation				
PROFILE NO:	VES 10	Amuda Opi-Agu		
Surface Elevation (m)		246		
S/N	Rho	Thick.(m).	Depth (m)	Elev(m
1	211.84	1.433	1.433	284.56
2	187.53	1.7516	3.1846	282.81
3	1773.4	13.96	17.1446	268.65
4	78.777	57.018	74.1626	211.83
5	156.31	83.523	157.686	128.31
6	83.483			

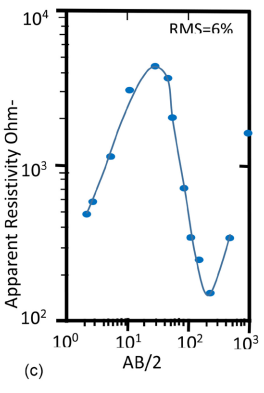

Resistivity Model Interpretation				
PROFILE NO:	VES 12	Amuda Opi-Agu		
Surface Elevation:		246		
S/N	Rho	Thick.	Depth	Elev
1	186.35	1.6604	1.6604	284.34
2	768	24.079	25.7394	250.28
3	33.17	30.572	56.3114	229.63
4	346.74	66.885	123.196	152.3
5	205.12	81.44	204.636	81.356
6	311.03			

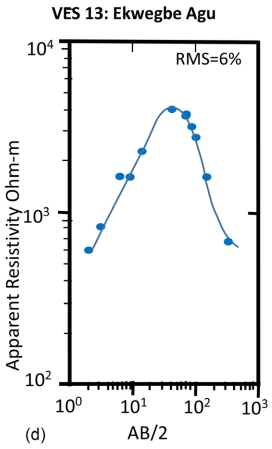

Resistivity Model Interpretation				
PROFILE NO:	VES 13	Ekwegbe Agu		
Surface Elevation:		246		
S/N	Rho	Thick.	Depth	Elev
1	477.75	1.7535	1.7535	284.24
2	5335.8	13.286	15.0395	270.35
3	524.31	42.103	57.1425	228.85
4	1261.2	66.043	123.186	152.8
5	205.12	81.447	204.633	81.356
6	1277.8			

Figure 5. (a)-(d) Resistivity sounding curve showing geo-electric parameters beneath VES 10 - 13 drawn within Mamu Formation in the northeastern and southeastern parts of the study area.

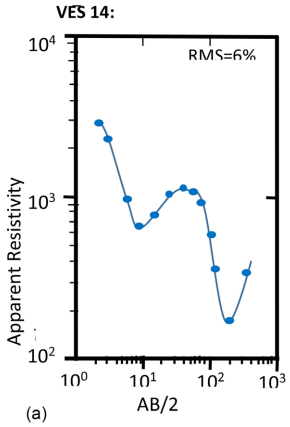

Resistivity Model Interpretation				
PROFILE NO:	VES 14			
Surface Elevation:		246		
S/N	Rho	Thick.	Depth	Elev
1	3577.7	1.7595	1.7595	242.24
2	371.19	4.6349	6.3944	237.61
3	1823.1	30.064	36.459	207.54
4	77.553	50.083	95.541	148.46
5	2305.7	124.55	220.09	23.91
6	1390.6			

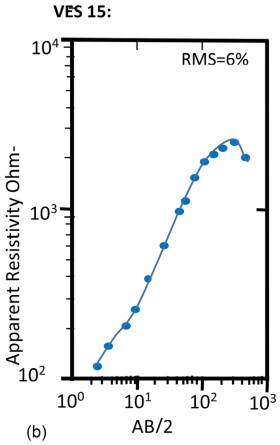

Resistivity Model Interpretation				
PROFILE NO:	VES 15			
Surface Elevation:		246		
S/N	Rho	Thick.	Depth	Elev
1	1092.4	1.7596	1.7596	344.24
2	2368.1	3.683	5.4526	340.55
3	33720	202.23	207.68	138.32
4	7351.9			
5	1092.4	1.7596	1.7596	344.24
6	2368.1	3.683	5.4526	340.55

Figure 6. (a) (b) Resistivity sounding curve showing geo-electric parameters beneath VES 14 - 15 drawn within Mamu Formation in the northeastern and southeastern parts of the study area.

3.2. Result of Hydrological Models of Aquifer Parameters

All the VES models obtained from resistivity sounding carried out within the Ajali Formation show a slightly close similarity in resistivity trend (an indication

of a uniform sub-surface condition) but differ in their layer thicknesses, a function of the variation in thickness of geo-electric layers along the profiles (Figure 4). The geo-electric parameters of the near-surface stratigraphy for ten soundings (VES 1, VES 7, and VES 8-15) drawn within the Mamu Formation are presented graphically in Figures 4-6. Whereas the results of the aquifer geo-electric parameters for the conventional Schlumberger spread at these sounding locations occupied within the study area are presented in Table 2.

4. Discussion

Evaluation of Aquifer Hydraulic Properties

In order to determine the hydrologic properties of the aquifer materials in the study area, contour maps showing the spatial distribution of aquifer resistivity, aquifer thickness, transverse resistance, transmissivity and hydraulic conductivity, were generated and analyzed.

Table 2. Aquifer geo-electric layer parameters obtained from the VES models (ND: No Data).

VES No.	Northing	Easting	Curve Type	No. of Geo-Electric Layers	Water Table (m) (Approx.)	Aquifer Thickness (m) (Approx.)	Aquifer Resistivity (Ωm)
1	6˚44'47.26"N	7˚29'30.22"E	AK	6	31	58	202.860
2	6˚45'12.02”N	7˚29'28.52”E	AK	6	22	85	110.050
3	6˚45'13.16"N	7˚28'14.41"E	HK	6	38	37	113.340
4	6˚46'12.42"N	7˚29'18.21"E	HK	6	30	133	1163.100
5	6˚44'14.18"N	7˚28'47.24"E	HK	6	13	42	56.079
6	6˚44'30.09"N	7˚28'09.43"E	HKA	6	35	60	129.420
7	6˚44'28.32"N	7˚29'50.89"E	QK	7	33	45	94.276
8	6˚44'30.29"N	7˚30'43.23"E	HK	6	14	68	429.730
9	6˚45'23.01"N	7˚30'45.03"E	KHQ	6	82	126	141.910
10	6˚45'27.09"N	7˚31'35.47"E	KHQ	7	81	79	51.475
11	6˚45'15.34"N	7˚29'50.29"E	K	6	74	57	78.777
12	6˚45'57.26"N	7˚29'0.16"E	KA	6	26	31	33.174
13	6˚44'40.11"N	7˚31'16.14"E	K	6	123	81	205.120
14	6˚46'34.48"N	7˚24'26.20"E	HKA	6	36	59	77.553
15	6˚43'56.20"N	7˚30'36.12"E	AK	4	208	ND	7351.900
16	6˚45'27.24"N	7˚28'20.09"E	AK	4	136	ND	2216.200
17	6˚45'21.14"N	7˚28'58.36"E	AK	4	136	ND	64.091
18	6˚45'52.41"N	7˚28'18.21"E	H	6	204	ND	33.884
19	6˚43'01.39"N	7˚30'35.06"E	H	6	123	81	45.667

4.1. Aquifer Geo-Electric Layer Parameters Obtained from the VES Models (ND: No Data)

With the exception of VES 1 and 15, VES 11 and 13, and VES 9-10, which show the AK, K and KHQ curve types, respectively, VES 7, 8, 12, 14 and 15 indicate types QK, HK, KA and HKA curves respectively (Table 2). The wide variation in curve types could be attributed to the variation in geo-electric characteristics of the sub-surface electro-stratigraphic units at these VES points, which is caused by the highly heterogeneous nature of the Mamu Formation in the study area.

Excluding VES 7, 10 and 15, all the VES models drawn within this formation display six geo-electric layers. VES 7 and 10 show seven geo-electric layers (Table 2). Of all the VES models having six geo-electric layers, VES 9, 12 and 13 are closely located and show similar trend in resistivity values (Figure 4, Figure 5). The six geo-electric layers that underlie VES 1 and VES 8 - 14 correspond to: lateritic overdurden, dark grey shale/siltstone, silty sandstone, siltstone, dark grey shale/clay and siltstone. However, in VES 11, the thin dark grey shale/clay sequence was not observed. In this case, a layer of silty sandstone was present beneath the siltstone unit that occupies the fourth geo-electric layer in this model. In the VES models, the resistivity range of the lateritic overburden varies between 186.38 and 3385.3 Ωm (see Figures 4-6). With the exception of VES 11 - 13, whose resistivities are 211.84 Ωm, 186.38 Ωm and 477.75 Ωm, respectively, the thin-dry overburden layer is characterized by high resistivity values. The low resistivity values observed in VES 11 - 13 (see Figure 5) could be attributed to the wetness of the near-surface at the VES stations during data acquisition. In VES 9, the lateritic overburden unit makes up the first and second geo-electric layers with a combined thickness of about 8.15 m. Conversely, the resistivity of the underlying dark grey shale/siltstone unit decreased in all the VES models except in VES 12 - 13. The low resistivities (155.89 - 711.21 Ωm) recorded in these other VES models is an indication that the dark grey shale/siltstone unit, which occupies the second geo-electric layer in the VES models (and third geo-electric layer in VES 9), is wet but not saturated. On the other hand, the lesser degree of wetness in VES 12 - 13 could be responsible for the higher resistivity values (768.42 - 5335.8 Ωm) observed in these VES models (Figure 5). The third geo-electric layer, which is clearly captured at depth of 3.14 to 15.71 m, represents the unsaturated zone within the silty sandstone sequence and is characterized by resistivity values that range from 497.51 to 6462.5 Ωm. In VES 9, this lithological sequence occurs at the fourth geo-electric layer (see Figure 4) whereas in VES 12, the entirety of the silty sandstone unit is saturated with fresh water, with the water table occurring at its topmost part (Figure 5). Beyond the unsaturated zone, a sharp decrease in resistivity is observed in all the VES models. In comparison with other geo-electric layers, this zone possesses the least resistivity values (51.475 - 205.12 Ωm) in all the models, and represents the fresh-water bearing aquifer beneath the VES stations. The aquifer thickness and depth ranges between 31 to 126 m and 14 to 123 m respectively (see Figures 4-6).

In all the VES models, this aquiferous zone occurs in the fourth geo-electric layer except in VES 9 and 12 where it occupies the fifth and third geo-electric layers respectively (see **Figure 4**, **Figure 5**). Generally, aquifer thickness within the Mamu Formation appears to increase eastwards away from the boundary between the Ajali and Mamu Formations (see **Table 2**).

Although this zone of saturation indicated a sharp resistivity drop and corresponds to the third geo-electric layer in VES 13, it is however, not adjudged to be the main aquifer beneath the VES model despite it being productive. The fifth geo-electric layer, by virtue of its resistivity (205.12 Ωm) and thickness (81.45 m), is considered a more prolific aquifer and is therefore recognized as the main aquifer beneath the VES station. The geological sequence that makes up this unit is siltstone. The high resistivity zone (1261.2 Ωm) overlying the main aquifer constitutes the vadose zone and occurs above the water table with a thickness of 66.05 m (see **Figure 5**). In other VES models (VES 1, 8 and 14), the siltstone layer underlies the aquiferous silty-sandstone interval, and is characterized by high resistivity values (1884.5 - 6103 Ωm) that depicts a dry zone. However, in VES 12, this zone shows evidence of saturation although the degree of saturation reduces downward as depicted by the increase in resistivity values (see **Figure 5**). In contrast, the downward decrease in layer resistivity as indicated by the siltstone unit in VES 9 and 11 suggests a downward increase in the degree of saturation from the overlying silty-sandstone aquifer (see **Figure 4**, **Figure 5**). The siltstone unit occupies the fifth geo-electric layer in VES 1, 8 and 14, the fourth and fifth geo-electric layers in VES 12 and the sixth geo-electric layer in VES 9 and 11. The basal layer comprising dark grey shales of high resistivity values (311.03 - 3661.0 Ωm) make up the sixth geo-electric layer in VES 1, 8 and 12 - 14. The high resistivities are an indication of a dry zone except in VES 12 where a low resistivity value is observed suggesting that the shales are probably wet beneath the VES station. This rock unit was not modelled in VES 9 and 11. VES 7 and 10 are also located within the Mamu Formation. Unlike the other VES models which have been previously described, they are characterized by seven geo-electric layers (see **Table 2**). Both VES models indicate similar resistivity trends and show a QK and KHQ curve types respectively. The geological sequences that make up these seven geo-electric layers are: lateritic overburden, dry dark grey shale/siltstone, wet dark grey shale/siltstone, unsaturated silty-sandstone, saturated silty-sandstone, siltstone and dark grey shale.

The thin overburden of laterite is characterized by high resistivity values that range from 712.52 to 2831.4 Ωm and a thickness of 1.66 m in both VES models (**Figure 4**, **Figure 5**). The second and third geo-electric layers constitute the same rock material, the dark grey shale/siltstone, but have contrasting resistivity values. The high resistivity (928.47 - 3124.6 Ωm) recorded in the second geo-electric unit is an indication of dry grey shale/siltstone whereas the low to moderate resistivity (120.23 - 243.89 Ωm) of the third geo-electric unit suggests that the lower section of the same shale/siltstone sequence is wet but not satu-

rated. Below this unit is a high resistivity layer (505.82 - 5180.8 Ωm) that represents the zone of infiltration (vadose zone) within the permeable silty sandstone unit (Figure 4, Figure 5). This interval comprises the fourth geo-electric layer in VES 7 and 10. Underneath the zone of infiltration is the fifth geo-electric layer that is characterized by low resistivity values in the range of 51.48 to 94.28 Ωm). This thick layer, which occurs within the silty-sandstone unit, is a fresh water bearing aquifer with a thickness that varies between 45.19 and 79.083 m. This zone is saturated with a good water bearing formation. The depth to the aquiferous zones ranges between 33 and 81 m (see Table 2). Underlying the groundwater aquifer in VES 7 are high resistivity materials (13,038 Ωm and 11,508 Ωm) interpreted as siltstone and dark grey shales (Figure 4). The high resistivity of these geological sequences, which occupy the sixth and seventh geo-electric layers, indicates that they are dry zones thereby suggesting a decrease in saturation downwards. In contrast, the resistivities of the siltstone and dark grey shales in VES 10 are considerable low (220.8 Ωm and 147.1 Ωm respectively; see Figure 5) implying that both geologic sequences underlying the aquifer are wet. This clearly shows a slight decrease and increase in saturation, respectively, as electrical drilling progressed from the siltstone unit to the shale horizon. In both VES curves, the thickness of the basal dark grey shale unit is undetermined (Figures 4(a)-(d), Figures 5(a)-(d)).

VES 15 is situated within the Mamu Formation, at the southern part of the study area (see Figure 6). The geological sequence beneath this VES station was inferred using the results of the borehole data due to their close proximity. Four geo-electric layers were recognized in this VES model, which show an AK curve type (see Table 2). The lithologic sequence that corresponds to these geo-electric layers are: lateritic overburden, dark grey shale/siltstone, silty sandstone and siltstone.

The first three geo-electric layers show a progressive increase in resistivity values downwards (Figure 5(c)). This is an indication of a downward increase in the degree of dryness, and in extension, a decrease in the degree of saturation. The resistivities of the first three geo-electric layers are 1092.4 Ωm, 2368.1 Ωm and 33,729 Ωm. From the ground surface, these layers terminate at depths of 1.76 m, 5.45 m and 207.68 m respectively. The drastic drop in the resistivity of the fourth geo-electric suggests that the siltstone sequence underlying the silty sandstone unit represents the aquiferous unit beneath VES 15. The depth to water (208 m) beneath VES 15 is the deepest when compared to other sounding models (Table 2). This could be attributed to the thickness of the infiltration zone (202.23 m) as well as the high elevation (346 m) at this VES point (Figure 6).

4.2. Discussion of Hydrological Models of Aquifer Parameters

4.2.1. Distribution of Aquifer Resistivity

The resistivity of the main aquifer units underlying the study area are generally low with values that vary between 1 and 500 Ωm especially at the western, cen-

tral and northeastern parts of the study area (Figure 7). These areas comprise the medium grain sandstone aquifer within the Ajali Formation as well as the silty sandstone and siltstone aquifers that occur in the Mamu Formation (see Figure 3). Of these areas, a small section of the northwestern fringes of the study area, west of VES 16 and 18 reveal a slightly higher aquifer resistivity within the Ajali Formation in the range of 100 to 2000 Ωm. VES 16 shows an aquifer resistivity of 2216 Ωm. Depths to water at VES 16 and 18 ranged between 136 and 205 m. Similarly, a slight increase in the resistivity (500 - 1000 Ωm) of the aquifers located within the Ajali and Mamu formation at the northwestern/north-central axis, was observed. The highest aquifer resistivities (2000 - 8000 Ωm) occurred within the Enugu Formation at the southeastern part of the study area where depths to the aquifer were observed to be higher (Figure 7). Most areas with shallow water depths were characterized by low aquifer resistivities and vice-versa. The higher resistivity of aquifers at greater depths could be attributed to increased compaction of the aquifer materials caused by the thickness of overlying sediments. Hence, the resistivity of aquifers is directly proportional to aquifer depth.

4.2.2. Distribution of Aquifer Depth

The deepest aquifers within the study area occur at the northwestern and southeastern parts, which are underlain by sediments of the Ajali and Enugu Formations, respectively (Figure 8). These areas are located in Umuile and west of Opi. Majority of the areas covering Ogbozara, as well as north and southwest of Opi are underlain by shallow aquifer systems.

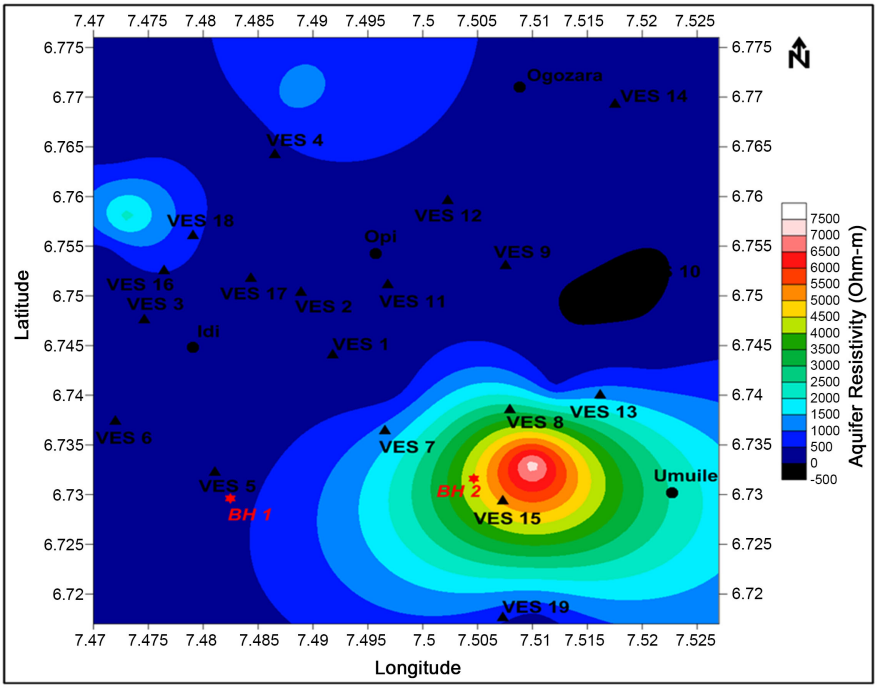

Figure 7. Contour map showing high aquifer resistivities predominantly at the southeastern region and partly at the northwestern region of the study area.

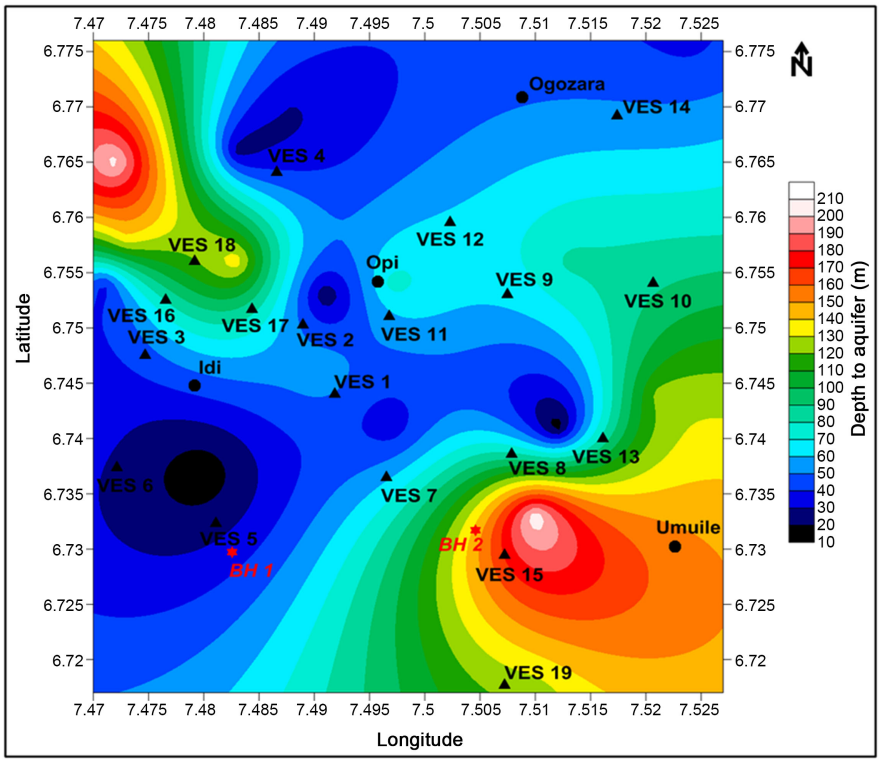

Figure 8. Contour map showing a progressive increase in aquifer depth towards the northwestern and southeastern directions which reflects the regional direction of groundwater flow and depicts a watershed.

Aquifer depths appear to increase progressively in the northwestern and southeastern directions, which correlate reasonably well with zones of higher aquifer resistivity (see **Figure 8**). Also, the direction of increasing aquifer depths coincides with the direction of decreasing elevation in the digital elevation model which supports a west to east direction of regional groundwater flow (see **Figure 2**). The increase in aquifer depths from the center of the study area to its northwestern part also indicates a possible direction of ground flow (**Figure 8**). This suggests that the study area is probably close to a watershed with two drainage areas located at the northwest and southeast of a cuesta that possibly trends in a roughly north of north-east to south of south-west (NNE-SSW) direction. Opi town appears to be close to the foot of the escarpment, southeast of the cuesta, with Unuile lying on the gentle area (plateau) (see **Figure 2**). The cuesta is the well-known Udi-Nsukka cuesta.

4.2.3. Distribution of Aquifer Thickness

Aquifer thickness increases from the southwestern to the northeastern part of the study area (**Figure 9**). The aquifer units in northwestern and southwestern axis varies between 30 and 65 m. Aquifer thickness at the southeastern section is moderate and ranges from 65 to 90 m. The thickness units of aquifer materials occur at the north-central and north-eastern part of the study area with a thickness that varies between 95 and 140 m (**Figure 9**). Most parts of the Ajali Formation

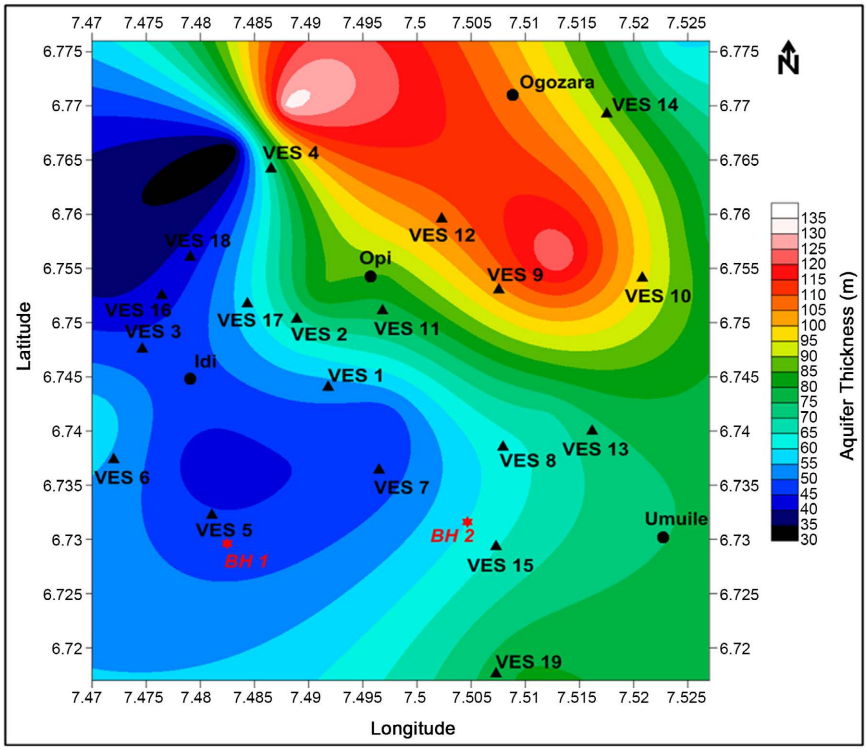

Figure 9. Contour map showing the increase in aquifer thickness from the southwestern part to the northeastern part of the study area.

especially at the western and southwestern regions have the lowest aquifer thicknesses. This is due to the generally lesser thickness of the Ajali Formation (compared to Mamu Formation) at these locations. However, the aquifer thickness model shows that a portion of the Ajali Formation within the north-western areas and west of Ogbozara possesses the thickness aquiferous interval (**Figure 9**). Most portions of the Mamu Formation particularly at the northcentral, northeastern and southeastern sections have the thickest aquifer units. Only the southwestern area of the Mamu Formation exhibits lesser aquifer thicknesses.

4.2.4. Distribution of Aquifer Hydraulic Conductivity and Transmissivity

The distribution of aquifer transmissivity and hydraulic conductivity in the study area are closely similar (**Figure 10** and **Figure 11**). Whilst aquifer transmissivity values vary between 1000 and 14,000 m^2/day, hydraulic conductivity values fall within the range of 5 to 50 m/day. The entire area shows transmissivity values that are suitable for ensuring very high groundwater yielding capacity except the northwestern fringes of the study area where lower transmissivity (0 - 500 m^2/day) and hydraulic conductivity values (<20 m/day) were also recorded (**Figure 10** and **Figure 11**). The northwestern axis is, therefore, only suitable for groundwater withdrawal of local or lesser commercial importance. According to Reference [22] aquifer transmissivity values that range from 10 to 1000 m^2/day have groundwater yielding capacity that can meet local demand and/or serve a very small community. High values of aquifer hydraulic conductivity and transmissivity are recorded at the north-central, northeastern and southeastern seg-

ments of the map that are underlain mostly by the Mamu and Enugu Formations. This suggests that the silty sandstone aquifer in the Mamu Formation transmits groundwater with a greater ease compared to the sandstone material in the Ajali Formation. Only a small section of area within the Ajali Formation recorded relatively higher aquifer transmissivity (4500 - 6000 m^2/day) and hydraulic conductivity values (45 - 65 m/day). This area lies west Opi and Ogozara (Figure 10 and Figure 11).

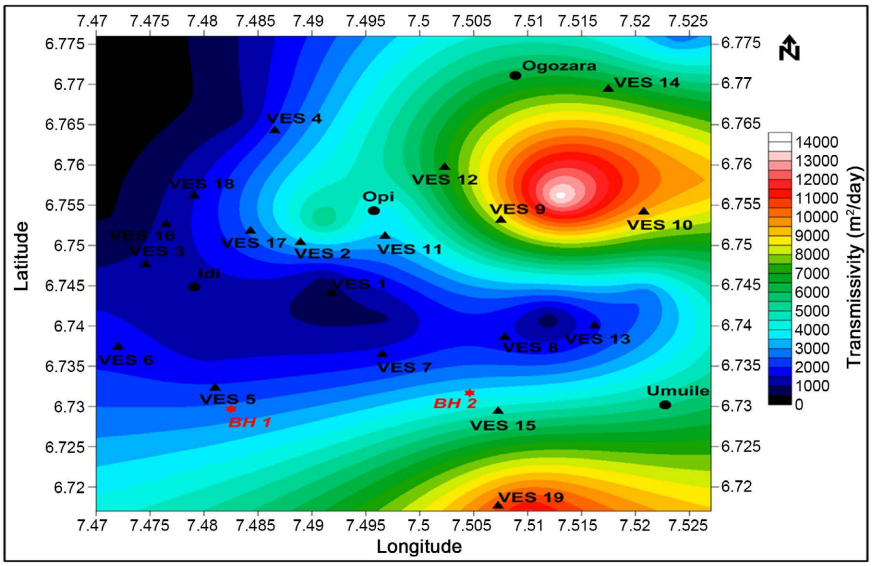

Figure 10. Contour map showing very high transmissivity values at the northeastern and southeastern parts of the study area.

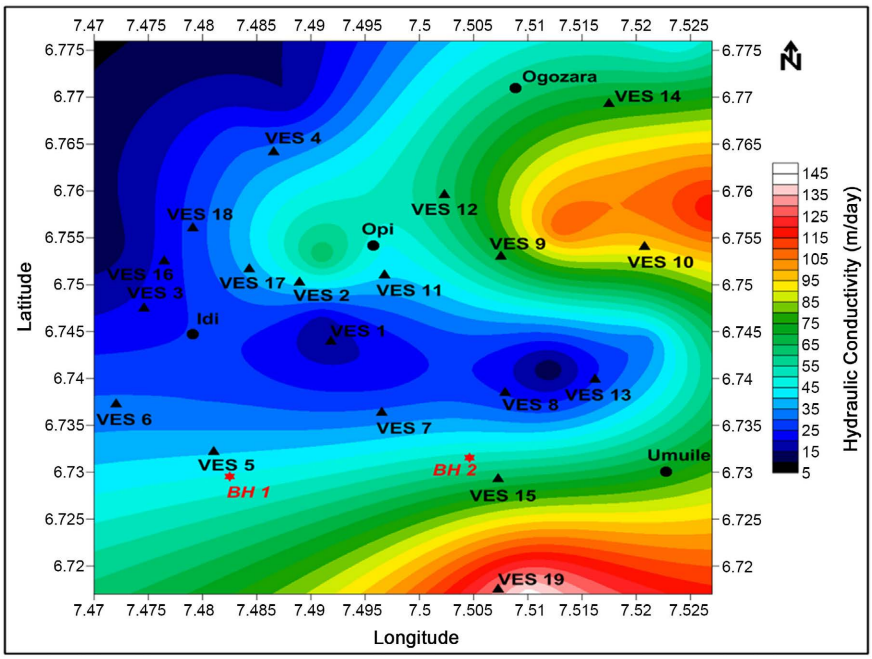

Figure 11. Contour map showing the spatial distribution of aquifer hydraulic conductivity values within the study area. Very high hydraulic conductivity values are also observed at the northeastern and southeastern parts of the study area.

4.2.5. Distribution of Aquifer Longitudinal Conductance and Transverse Resistance

The variation in aquifer longitudinal conductance within the study area follows similar pattern with the variation in aquifer transmissivity and hydraulic conductivity (Figure 12) with some minor exceptions. A slight homogeneity in the distribution of longitudinal conductance exists at the noth-central, northeastern and central portions of the study area where mainly low aquifer longitudinal conductance (0.1 - 0.7 Ω^{-1}) values were recorded. A NW-SE strip of moderate aquifer longitudinal conductance values, stretching northeast of Opi, is observed around VES 4, 17 and 18 with values that range from 0.8 to 0.9 Ω^{-1} (Figure 12).

The high conductance values could imply that the groundwater at the northeastern and southeastern areas posseses higher saline content compared to other areas. Fresh water bearing aquifer are more likely to occur at the central and north-central extremities of the study area where lower aquifer longitudinal conductance values are recorded. In some areas, the values of aquifer longitudinal conductance varied inversely to those of aquifer resistivity in the same areas. This is especially true for the northeastern, southwestern and partly the northwestern parts of the study area (Figure 7 and Figure 12).

Low values of aquifer transverse resistance occur at the central, southern and western regions of the study area (Figure 13). Only the northern end of the study area reveals moderate and very high values of transverse resistance (40, 000 to 170,000 Ωm^2) which are typical of very prolific aquifers.

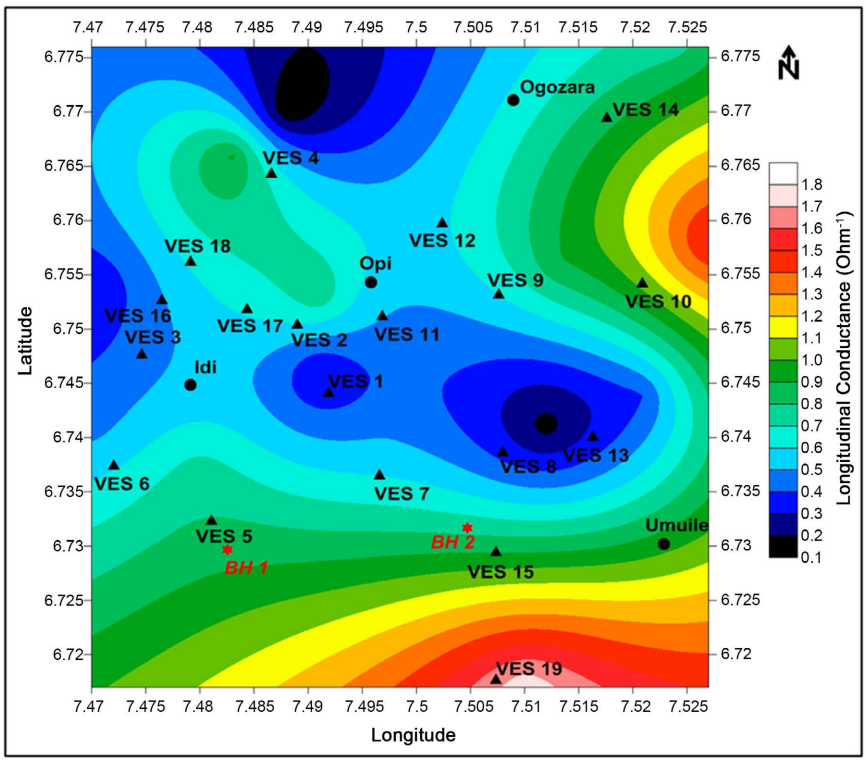

Figure 12. Contour map showing the spatial variation in aquifer longitudinal conductance, which is closely similar to the spatial distribution of aquifer hydraulic conductivity and transmissivity in the study area.

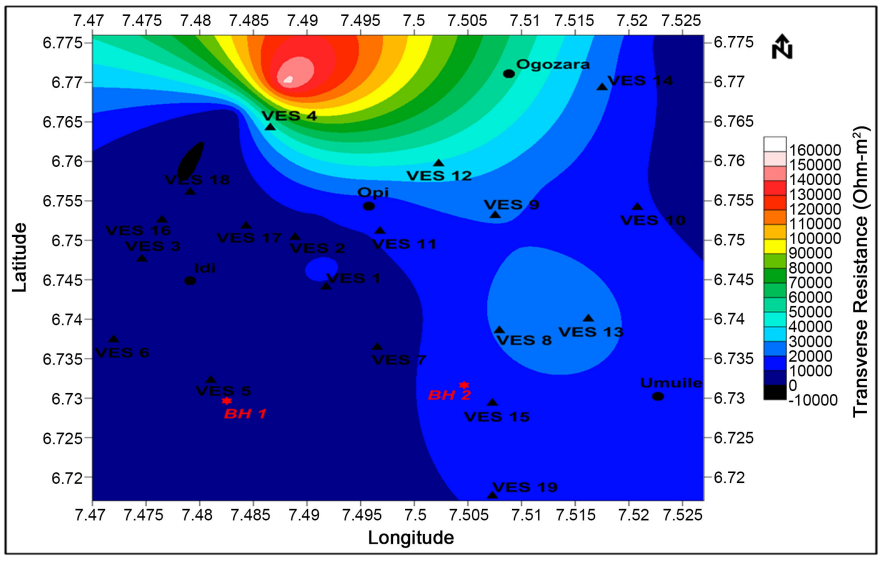

Figure 13. Contour map showing the distribution of aquifer transverse resistance in the study area.

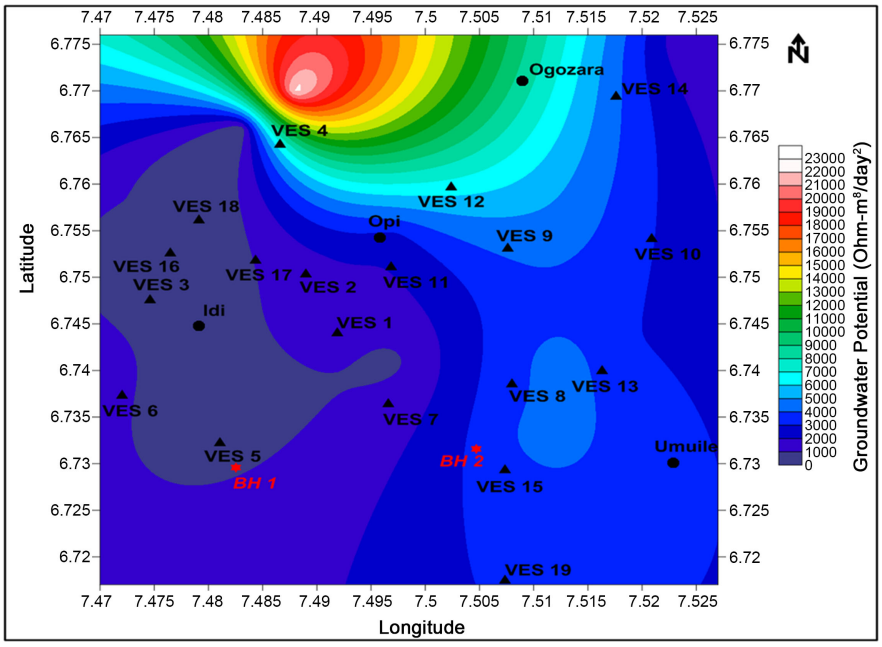

Figure 14. Groundwater potential map showing areas of high, intermediate and low potential for groundwater resources.

4.3. Hydrogeological Zonation

In demarcating the study area into groundwater potential zones, the various maps (transmissivity, hydraulic conductivity, longitudinal conductance, depth, thickness and resistivity) showing different aquifer hydraulic property distribution in the study area were overlaid to produce a groundwater potential map for the study area. The aim is to assess the sub-surface lithology suitable for low, intermediate or high groundwater potentials and hence, determine the area(s) that is best fit for borehole placement.

The generated groundwater potential map is displayed in Figure 14. The north-western part of the study area underlain partly by the Ajali and Mamu Formations, and situated west of Ogbozara and north of Opi shows the highest groundwater potential in the study area. The aquifer materials underlying this area is characterized by low resistivity, shallow depth, thick beds, moderate transmissivity and hydraulic conductivity, low longitudinal conductance and high transverse resistance.

5. Conclusion

The investigation of the hydrologic parameters at Ogbozara/Ekwegbe-Agu and the Environ using Dar-Zarrouk parameters has shown good result. After performing the investigation, the corresponding results show that the dominant curve type obtained from the different formations is the AK curve type followed by the HK curve type. The hydraulic conductivity in the area ranges from 5 m/day to 50 m/day, while the transmissivity values range from 1000 m^2/day to 14,000 m^2/day. The aquifer resistivity in the study area ranges from 1 Ωm to 500 Ωm. The depth to the water table range from 13 m - 20 8 m with a mean value of 76.05 m, while aquifer thickness varies between 95 m and 140 m with a mean value of 102.89 m. The values of the Dar-Zarrock parameters revealed that the transverse resistance varies between −10,000 Ωm^2 to 170,000 Ωm^2, while the longitudinal conductance varies from 0.1 Ω^{-1} to 1.9 Ω^{-1}. From the generated groundwater potential map of the study area, the north-western part of the study area underlain partly by the Ajali and Mamu Formations, shows the highest groundwater potential in the study area.

Acknowledgements

The authors acknowledge, with thanks, the efforts of the crew members of Felgra Links Nigeria Limited during the surface geophysical data acquisition and for providing the borehole logging data used for this study.

Conflicts of Interest

The authors declare no conflicts of interest regarding the publication of this paper.

References

[1] Ekwe, A.C., Onu, N.N. and Onuoha, K.M. (2006) Estimation of Aquifer Hydraulic Characteristics of Aquifer Hydraulic Characteristics from Electrical Sounding Data: A Case of Middle Imo River Basin Aquifers, South Eastern Nigeria. *Journal of Spatial Hydrology*, **6**, 121-132.

[2] Ezeh, C.C. (2011) Geoelectrical Studies for Estimating Aquifer Hydraulic Properties in Enugu State, Nigeria. *International Journal of Physical Sciences*, **6**, 3319-3329.

[3] Maillet, R. (1947) The Fundamental Equations of Electrical Prospecting. *Geophysics*, **12**, 529-556. https://doi.org/10.1190/1.1437342

[4] Onuoha, K.M. and Mbazi, F.C.C. (1988) Aquifer Transmissvity from Electrical

Sounding Data: The Case of the Ajali Sandstone Aquifers South-West Enugu, Nigeria. In: Ofoegbu, C.O., Ed., *Groundwater and Mineral Resources of Nigeria*, Friedrich Vieweg & Sohn, Braunchweig/Wiesbaden, 17-30.

[5] Ezeh, C.C. (2012) Hydrogeophysical Studies for the Delineation of Potential Groundwater Zones in Enugu State, Nigeria. *International Research Journal of Geology and Mining*, **2**, 103-112.

[6] Okonkwo, A.C. and Ezeh, C.C. (2013) Aquifer Hydraulics and Delineation of Groundwater Quality Zones Using Electrical Resistivity Method at Oduma and Environs in Enugu State, Southeastern Nigeria. *Journal of Geology and Mining*, **3**, 31-39.

[7] Ekwe, A.C., Nnodu, I.N., Ugwumbah, K.I. and Onwuka, O.S. (2010) Estimation of Aquifer Hydraulic Characteristics of Low Permeability Formation from Geosounding Data: A Case Study of Oduma Town, Enugu State. *Journal of Earth Sciences*, **4**, 19-26. https://doi.org/10.3923/ojesci.2010.19.26

[8] Udoinyang, I.E. and Igboekwe, M.U. (2012) Aquifer Transmissivity, Dar Zarrouk Parameters and the Direction of Flow of Suspended Particulate Mattee in Boreholes in MOUAU and the Kwa Ibo River Umudike-Nigeria. *Greener Journal of Physical Sciences*, **2**, 70-84.

[9] Chandra, S., Ahmed, S., Ram, A. and Dewandel, B. (2008) Estimation of Hard Rock Aquifers Hydraulic Conductivity from the Geoelectrical Measurements: A Theoretical Development with Field Application. *Journal of Hydrology*, **357**, 218-227. https://doi.org/10.1016/j.jhydrol.2008.05.023

[10] Laouini, G., Etuk, S.E. and Agbasi, O.E. (2017) Delineation of Aquifers Using Dar Zarrouk Parameters in Parts of Akwa Ibom, Niger Delta, Nigeria. *Journal of Hydrogeology and Hydrologic Engineering*, **6**, Article No. 18.

[11] Kelly, W.E. and Frohlich, R.K. (1985) Relations between Aquifer Electrical and Hydraulic Properties. *Groundwater*, **23**, 182-189. https://doi.org/10.1111/j.1745-6584.1985.tb02791.x

[12] Okiongbo, K.S. and Oborie, E. (2015) Investigation of Relationships between Geoelectric and Hydraulic Parameters in a Quaternary Alluvial Aquifer in Yenagoa, Southern Nigeria. *Ife Journal of Science*, **17**, 163-172.

[13] Ladipo, K.O., Nwajide, C.S. and Akande, S.O. (1992) Cretaceous and Paleogene Sequences in the Abakaliki and Anambra Basins, Southeastern Nigeria, A Field Guide. International Symposium on the Geology of Deltas, Porthacourt, 39.

[14] Reyment, R.A. (1964) Review of Nigerian Cretaceous—Cenozoic Stratigraphy. *Journal of Nigerian Mining, Geology and Metallurgical Society*, **1**, 61-80.

[15] Reyment, R.A. and Morner, N.A. (1977) Cretaceous Transgressions and Regressions Exemplified by the South Atlantic. *Paleontological Society of Japan*, **21**, 247-260.

[16] Reyment, R.A. (1965) Aspect of the Geology of Nigeria. University of Ibadan Press, Ibadan, 145.

[17] Obi, G.C. (2000) Depositional Model for the Campanian-Maastrichtian Anambra Basin, Southern Nigeria. Ph.D. Thesis, University of Nigeria Nsukka, Enugu, 291.

[18] Kogbe, C.A. (1989) The Cretaceous and Paleogene Sediments of Southern Nigeria. In: Kogbe, C.A., Ed., Geology of Nigeria, 2nd Edition, Rockview Nigeria Limited, Lagos, 273-286.

[19] Nwajide, C.S. (1990) Cretaceous Sedimentation and Paleogeography of the Central Benue Trough. In: Ofoegbu C.O. (Ed.), *The Benue Trough, Structure and Evolution*, Friedrich Vieweg & Sohn, Braunchweig/Wiesbaden, 19-38.

[20] Lowrie, W. (2007) Fundamentals of Geophysics. Cambridge University Press, Cambridge, 392. https://doi.org/10.1017/CBO9780511807107

[21] Zohdy, A.A.R., Eaton, G.P. and Mabey, D.R. (1974) Application of Surface Geophysics to Groundwater Investigations. In: Keller, G.V. and Frischnechk, F.C., Eds., *Techniques of Water Resources Investigations of the United States Geological Survey*, United States Government Printing Office, Washington DC, 12-26.

[22] Kearey, P., Brooks, M. and Hill, I. (2002) An Introduction to Geophysical Exploration. 3rd Edition, Blackwell Science, Oxford, 262 p.